Simultaneous Thermal Imaging of Peltier and Joule Effects

B. Vermeersch and A. Shakouri

Baskin School of Engineering, University of California at Santa Cruz
1156 High Street SOE2, Santa Cruz CA 95064 – Email: bvermeer@soe.ucsc.edu

Abstract

We present a novel thermoreflectance technique to visualise quasi-static Peltier and Joule thermal distributions simultaneously, enabling side-by-side comparison in situ. The main principle is an extension of so called '4-bucket' imaging techniques well documented in the literature. The method is particularly advantageous in improving both the reliability and turnaround time for the characterisation of thermoelectric materials and related devices such as microcoolers.

In essence, separation of Peltier and Joule effects relies on their respective linear and quadratic current dependence. Established techniques employ two distinct runs of data averaging: one with forward and one with reverse supply polarity. Post processing of the two images provides the Peltier and Joule terms, based on the sign change induced to the former. In practice however, the polarity switch often gives rise to issues with probing and modified contact resistance. Sample movement and drifting lab conditions also introduce asymmetry into the runs, further distorting the measurement. Finally, the experimenter must wait for full completion of both runs to obtain actual results.

The key to the proposed technique is that a bipolar excitation is used. Namely, we supply a slow sine wave with zero offset to the DUT. This causes the Peltier term to manifest itself in the first temperature harmonic, while the Joule term has a second harmonic component. A phase-locked CCD oversamples the signal 8 times (instead of 4) per period. Appropriate image processing yields magnitude and phase distributions for both harmonics, as well as the DC component. The method thus provides immediate and simultaneous access to the Peltier and Joule terms, and enables real-time fine tuning of the experiment if necessary. Validation against the unipolar approach shows a nearly perfect match. Characterisation of a heater and p-type thermoelectric sample further illustrates the technique.

Key words: thermal imaging, thermoreflectance, Peltier/Joule, thermoelectrics

1 Introduction

Thermoreflectance based methods are a well established means for thermal imaging of microelectronic structures and devices. Thermal distributions with temperature resolution well below 50 mK can be obtained at submicron spatial resolution. A variety of methods is available to study either the quasi-static, transient or frequency domain behaviour. Essentially the core principle remains the same. The measurement is based on the small but detectable temperature dependence of the optical reflectivity of the sample under study, characterised by the thermoreflectance coefficient C_{TR}. A detailed overview of CCD based thermoreflectance techniques can be found in [1].

Typical C_{TR} values are so small that the difference between the 'hot' image (DUT in on state) and 'cold' image (DUT idle) is close to or even below the noise floor of the imaging system. Lock-in techniques must be employed to resolve the small variation and reconstruct the thermal signal. For quasi-static regimes, as we will deal with here, a so called '4-bucket' approach [2] is commonly used. The main principle is schematically shown in Fig. 1a. An offset sine wave drives the DUT, such that the excitation current is of the form

$$I_{\mathrm{DUT}} = I_0 \left[1 + \cos(2\pi f\, t)\right] , \qquad (1)$$

which creates an oscillating temperature field. In turn, this introduces a small sinusoidal component

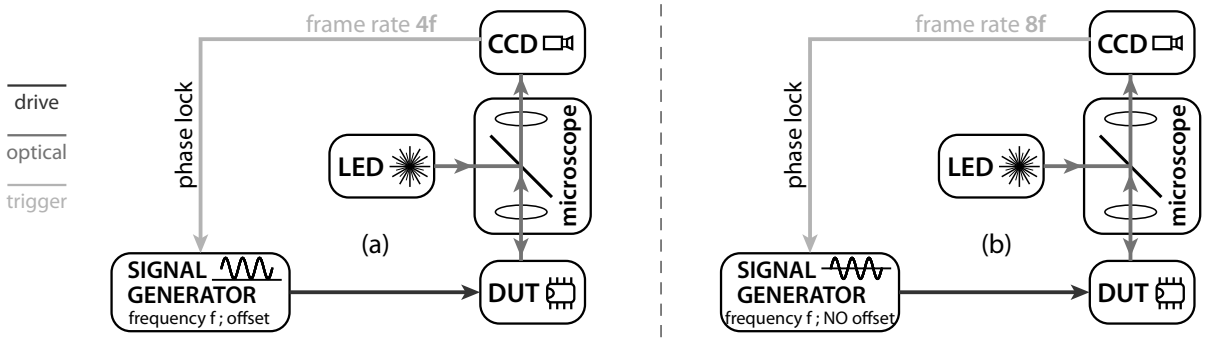

Figure 1: Schematic principle of quasi-static thermoreflectance imaging: (a) established '4-bucket' technique, (b) proposed '8-bucket' technique.

with amplitude R_1 and relative phase ϕ in the optical reflectivity of the sample, superimposed on the reference value R_0. A phase-locked CCD camera running at frame rate $4f$ captures the light being reflected under continuous wave illumination. By keeping the shutter open for the duration of each frame, quarter period integrals of the signal are obtained. These 4 data containers (the 'buckets') are then averaged for many cycles to achieve a sufficient signal-to-noise ratio (SNR). Adequate processing of the 4 acquired images enables to extract the reflectivity parameters R_0, R_1 and ϕ and yields the temperature distribution through

$$\Delta T(x,y) = \frac{R_1(x,y)}{C_{TR}(x,y)\cdot R_0(x,y)}\,. \qquad (2)$$

2 Thermal Imaging of Thermoelectrics

2.1 General Background

In most common electronic systems, self heating arises due to Joule dissipation induced by one or more electrical loss mechanisms. Thermoelectrics are somewhat special in the sense that some device areas show dominant appearance of Peltier effects, which are crucial to their working. An increasing amount of attention is being dedicated to this class of materials given some of their promising potential for energy conversion and thermal management [3]. Thermoelectric modules are being investigated as a potential means to generate electricity from waste heat in e.g. automotive applications as well as to provide highly efficient household heating and cooling systems [4]. Microrefrigerators can be used to address localised hot spots on a chip [5]. Along with other characterisation techniques, thermal imaging is a useful tool to assess the performance and assist improvement of these materials and derived devices. Although basic information can be obtained from just observing the net temperature that results from the superposition of the competing Peltier and Joule effects, the desire emerges to study both of these terms individually.

2.2 Established Approach: Two Unipolar Runs

The ability to separate the two effects is based on how they evolve with the supplied current. The Peltier term has a linear dependence, while the Joule term scales quadratically. In a microcooler, for example, we could roughly estimate the net temperature rise relative to ambient as:

$$\Delta T = a\, I_{\mathrm{DUT}} + b\, I_{\mathrm{DUT}}^2 \qquad (3)$$

This intuitive relation is confirmed by both theoretical and experimental analyses yielding characteristics of this form [5]. The first term ($a < 0$) in (3) represents the desired Peltier cooling while the second one ($b > 0$) embodies the residual Joule losses. Note that the coefficients a and b will strongly vary throughout the sample depending on the position with respect to the active region.

Running two distinct measurements, namely one with forward and one with reverse current polarity ($I_{\mathrm{rev}} = -I_{\mathrm{fw}}$), enables extraction of the Peltier and Joule distributions:

$$\Delta T_{\mathrm{P}}(x,y) = \frac{\Delta T_{\mathrm{fw}}(x,y) - \Delta T_{\mathrm{rev}}(x,y)}{2}$$
$$\Delta T_{\mathrm{J}}(x,y) = \frac{\Delta T_{\mathrm{fw}}(x,y) + \Delta T_{\mathrm{rev}}(x,y)}{2} \qquad (4)$$

We note that the presence of phase terms actually necessitates data processing more elaborate than suggested by (4) to obtain the desired Peltier and Joule terms. Mathematical details are beyond the scope of this discussion and, in addition, do not affect the general measurement principle. In essence, the system locks into the first temperature harmonic and observes a superposition of Peltier and Joule effects.

The main issue is that their separation is solely based on the sign change of the Peltier term upon polarity reversal. Any asymmetry between the two runs will render improper results. In certain cases, wire connections must be physically altered to reverse the current polarity. This elevates the chance of movement of the supply probes and/or the DUT itself. The former event will likely alter the electrical contact resistance, leading to current imbalance ($I_{\text{rev}} \neq -I_{\text{fw}}$), while the latter further distorts the data manipulation since $(x, y)_{\text{fw}} \neq (x, y)_{\text{rev}}$. In addition, thermal distributions become only available at the very end of the experiment after post-processing. Averaging times exceeding one hour are not uncommon.

2.3 Proposed Technique: One Bipolar Run

An alternative method is desirable to overcome these issues. The technique we propose here no longer requires manipulation during the experiment while providing real-time access to intermediate results. The key difference is to remove the offset from the excitation signal, using a pure sine wave instead:

$$I_{\text{DUT}} = I_0 \cos(2\pi f\, t) \tag{5}$$

Considering (3), the Peltier term will manifest itself at the first temperature harmonic, while the Joule term has a DC and second harmonic component. The surface reflectivity of the DUT can be written as (omitting the (x, y) dependences to simplify the notation):

$$R(t) = R_0 + R_1 \cos(2\pi f\, t + \varphi) + R_2 \cos(4\pi f\, t + \psi) \tag{6}$$

R_1 and R_2 are proportional to aI_0 and $\frac{1}{2}bI_0^2$ respectively, while φ and ψ represent the thermal inertia (as observed at the surface) associated with their respective Peltier and Joule terms. Note we cannot assume these phase shifts to be automatically equal since the associated physical mechanisms occur at disparate frequencies and may originate from different depths in the sample. Full data reconstruction requires the fastest term to be oversampled four times, leading to an 8:1 detector-to-excitation rate. We illuminate the DUT with a constant, uniform optical flux Φ and run the CCD at frame rate $8f$ (Fig. 1b). This yields eighth-period integrals of the reflected signal $s(t) = \Phi \cdot R(t)$:

$$K_n = \int_{(n-1)\frac{T_s}{8}}^{n\frac{T_s}{8}} s(t)\mathrm{d}t \qquad n = 1 \dots 8 \tag{7}$$

with K_n the n-th image in the cycle and $T_s = \frac{1}{f}$ the period of the oscillating signal. In what follows, we can omit the optical flux Φ since it is a common factor to all images and does not affect the results upon processing. The background reflectivity can be readily reconstructed as:

$$R_0 = \frac{1}{T_s} \sum_{n=1}^{8} K_n \tag{8}$$

This DC term serves as normalisation factor to convert the reflectivity data to temperature values, i.e.

$$\Delta T_{\text{Peltier}} = \frac{R_1}{C_{TR} \cdot R_0}; \Delta T_{\text{Joule}} = \frac{R_2}{C_{TR} \cdot R_0}\,. \tag{9}$$

For notation purposes, let us define

$$\begin{cases} L_n = K_n - K_{n+4} \\ M_n = K_n + K_{n+4} \end{cases} \quad (n = 1 \dots 4)\,. \tag{10}$$

One can prove the remaining unknown signal parameters can be extracted as:

$$R_1 = \frac{\pi \sqrt{L_1^2 + L_2^2 + L_3^2 + L_4^2}}{\sqrt{2} \cdot \sqrt{2 - \sqrt{2}} \cdot T_s} \tag{11}$$

$$\varphi = -\arctan\left(\frac{L_1 + L_2 + L_3 + L_4}{L_1 + L_2 - L_3 - L_4}\right) \tag{12}$$

$$R_2 = \frac{\pi}{\sqrt{2}\, T_s} \sqrt{(M_1 - M_3)^2 + (M_2 - M_4)^2} \tag{13}$$

$$\psi = -\arctan\left(\frac{M_1 + M_2 - M_3 - M_4}{M_1 - M_2 - M_3 + M_4}\right) \tag{14}$$

This fully and simultaneously characterises the magnitude and phase distributions of the separated Peltier and Joule terms as desired.

We wish to mention we earlier reported on a heterodyne technique enabling separation of Joule and Peltier effects in transient mode [6], although the system can only resolve one term at the time instead of both simultaneously. This transient method features pulsed illumination which substantially increases the complexity of the system. It also requires excitation frequencies of at least a couple of hundred Hz and is therefore not applicable to static regimes.

3 Experimental Results

3.1 Validation of the Method

In order to validate our method experimentally, we have performed thermal imaging with subsequently the proposed and established technique on the same sample. The DUT is a SiGe microrefrigerator, with active area of about 40×40 microns. A function generator at $f = 3.75$ Hz provides an oscillating voltage used as bias and delivers a peak current $I_{\max} \approx 191$ mA to the cooler. For either technique, a total of 3200 images (equivalent to 400 effective averaging cycles) are processed. Both experiments had a run time of about 25 minutes. An uncalibrated, uniform estimate of $C_{TR} = 2 \times 10^{-4}\,\mathrm{K}^{-1}$ is used in (9) for reflectivity to temperature conversion. The results are summarised in Figure 2. The obtained distributions are matching very well except for two main disparities that require clarification.

The first difference is the obvious mismatch in the phase of the Joule component. The main characteristics, however, are clearly preserved: sharp contrasts appear in the same locations. A closer inspection reveals the two distributions only differ by a constant offset. Figure 3 compares the two images again after offsetting our data uniformly by 90 degrees. The distributions now become very similar. The phase shift can be easily attributed to the fact that the systems provide only relative phase information i.e. with respect to the carrier of the oscillating signal. Since our method captures the Joule term at the second harmonic of the

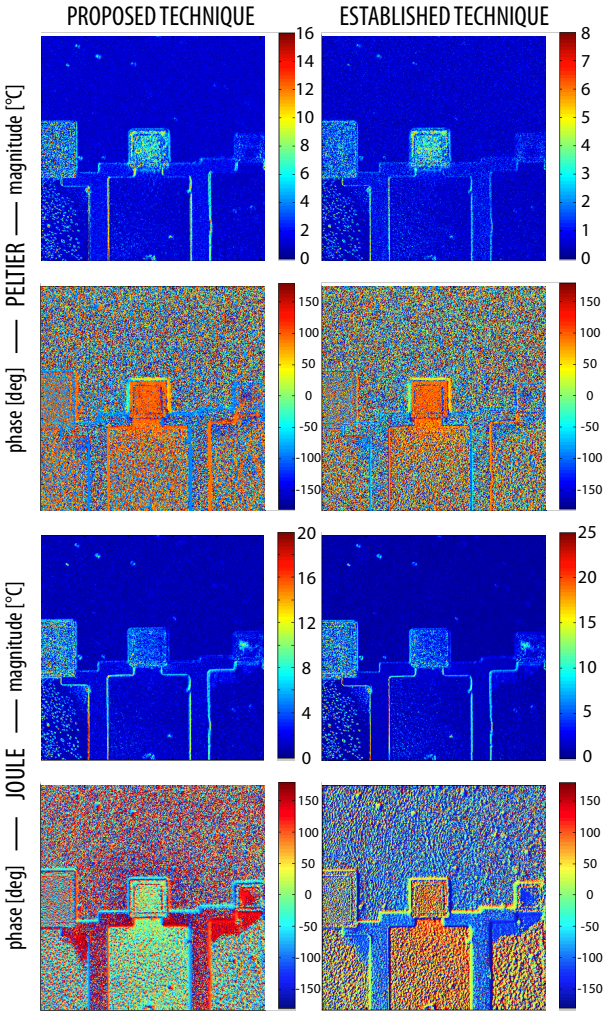

Figure 2: Cross-validation of the proposed method (one bipolar run, left) versus established method (two unipolar runs, right) for thermal imaging of Peltier and Joule distributions. Only the center cooler is biased.

driving signal while the unipolar approach observes the first, the phase is determined against a different reference. The frequency dependence of the thermal inertia can introduce an additional dis-

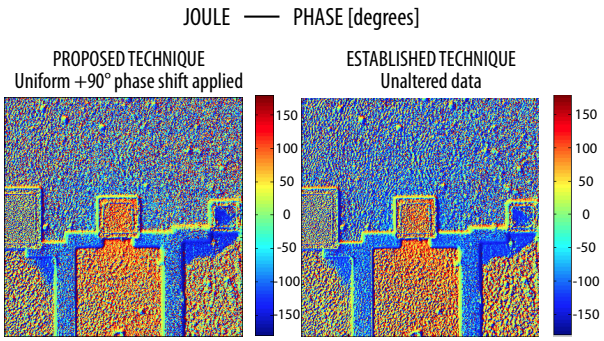

Figure 3: Additional validation of the phase of the Joule term after offset correction.

crepancy. This effect, however, is usually very minor given the relatively quick response of most samples with respect to the slow modulation. It is important to note that phase is a relatively complex quantity that is highly sensitive to system noise and accurate timing. Obtaining good agreement (both for Peltier and Joule terms) is non-trivial and a profound means of validation.

Secondly, a closer look at the magnitude distributions in Fig. 2 shows that although the images have a very similar appearance, they differ quantitatively. The Peltier and Joule terms observed by our method deviate from the reference data by a factor of 2 and 0.8 respectively. This mismatch in signal strength can also be easily explained. Though the same peak current I_{max} was used in both experiments, the thermal power being induced is not equivalent. Under bipolar exciation, i.e. $I_{\mathrm{bi}} = I_{\mathrm{max}} \cos(2\pi f\, t)$, the oscillating Peltier and Joule components scale as aI_{max} and $\frac{1}{2} bI_{\mathrm{max}}^2$ respectively. For the unipolar case, where $I_{\mathrm{uni}} = \pm\frac{I_{\mathrm{max}}}{2}[1 + \cos(2\pi f\, t)]$, the magnitude of the first harmonic becomes $\pm\frac{1}{2} aI_{\mathrm{max}} + \frac{5}{8} bI_{\mathrm{max}}^2$. This indeed leads to relative ratios of 2:1 (Peltier) and 4:5 (Joule) as observed in the images. In order to meet expectactions intuitively prompted by a quasi-static technique, it is preferable for the system to produce images that are compatible with those that would be obtained under actual steady state conditions $I_{\mathrm{DC}} = I_{\mathrm{max}}$. This is readily achieved by applying appropriate correction factors to (9), namely 1 for Peltier and 2 for Joule.

Finally, let us go briefly over the measurement itself. A clear Peltier signal is visible over the central cooler surface, as expected. Active areas can be easily identified by a clear phase contrast with the substrate background. Besides the actual DUT, we also observe thermal signals in the surrounding, unbiased devices. This makes us strongly believe that the sample is behaving erroneously and likely damaged. The Joule term, and the phase image in particular, suggests that current is leaking away from the bias electrode to other areas of the sample. In addition, the bright spot in the small cooler on the right probably indicates a defect in the SiGe superlattice, offering a quasi-short between top contact and ground plane.

3.2 Integrated Microheater

We have used our technique to obtain thermal images of a microheater sample. The DUT roughly measures 60 by 60 microns and consists of a serpentine gold resistor patterned on top of a thermoelectric microcooler. Only the heater is biased, at a frequency of 3.75 Hz (CCD frame rate 30). The uncalibrated magnitude data (i.e. employing a uniform C_{TR} value) is presented in Fig. 4.

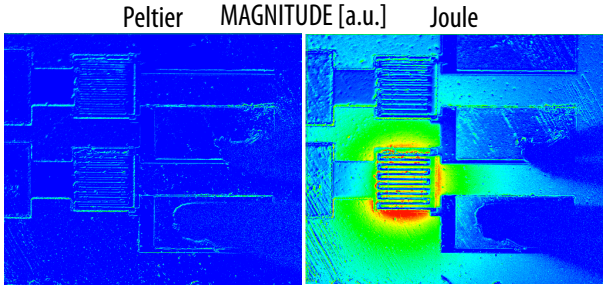

Figure 4: Thermal magnitude images of a microheater.

Apart from spurious device contours (a typical feature induced by optical scattering at sharp edges and interfaces), no detectable signal appears in the Peltier image, as appropriate. This provides another baseline verification of our methodology. Joule heating, on the other hand, is clearly visible at and in the wide vicinity of the heater. The observed pattern indicates a near-radial heat spreading into the substrate. Note that the signal over the active area, where the highest temperatures should be expected, is notably small. This is most likely caused by a weak thermoreflectance coefficient of the involved materials under the blue illumination ($\lambda \approx 460$ nm) used in the experiment.

3.3 Bulk p-Type Thermoelectric

As a final example, we investigated a test structure used for characterisation of thermoelectric materials. The sample consists of a substrate (the material under test) with a passivating (insulating) film on top. A rectangular window is etched into the passivation and filled with gold. Finally an electrode is deposited on top of the sample to bias the material. From the injection window, the current spreads into the substrate and is then collected again in the ground plane at the bottom. The layout of the sample is illustrated in Fig. 5a.

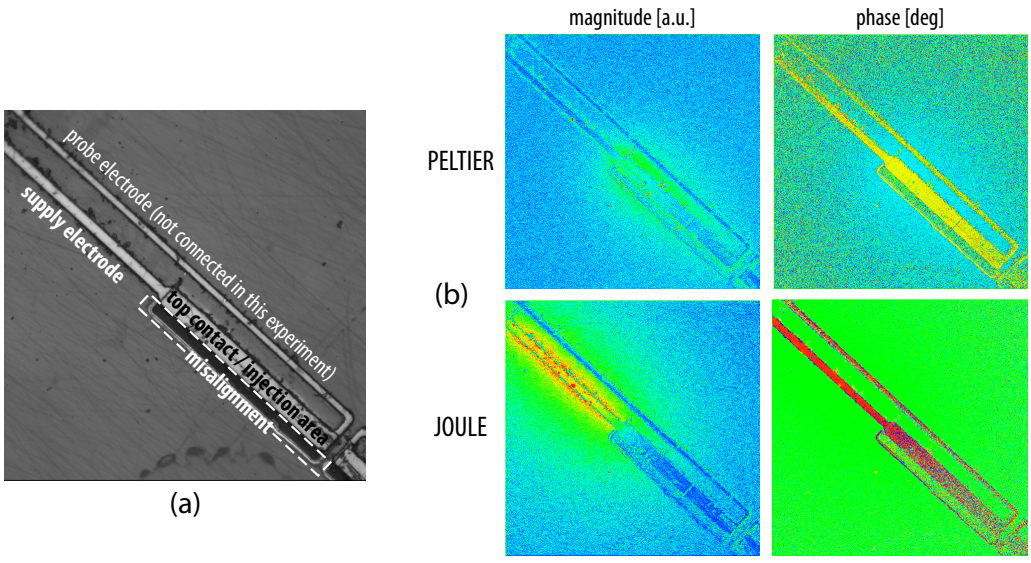

Figure 5: Thermoelectric characterisation sample: (a) physical layout, (b) obtained Peltier and Joule distributions.

We note that a fabrication error rendered the effective injection window of this particular sample smaller than usual: the top electrode is not properly aligned to the passivation etch (Fig. 5a).

Figure 5b presents some exemplary thermal images. We observe a dominant Peltier component near the current injection window, as expected. The 'halo' around the top contact, particularly visible in the phase image, results from superimposed thermal diffusion and active contributions from the bulk. Joule effects originate mainly from the losses in the relatively narrow supply electrode. As the current reaches the injection window, it gradually flows into the substrate. The dissipated power density in the top contact drops accordingly, as confirmed by the increasingly noisy phase signal in the direction of the current flow.

4 Conclusions

We presented a quasi-static thermoreflectance technique allowing simultaneous imaging of Peltier and Joule effects. It is based on the harmonic separation of the two components upon purely sinusoidal excitation of the DUT. Our single-run approach improves experimental robustness and provides real-time access to the thermal distributions, as opposed to established methods requiring two distinct runs with opposite current polarity and data post-processing. Cross-validation yields a nearly perfect match.

References

[1] M. Farzaneh, K. Maize, D. Luerssen, J.A. Summers, P.M. Mayer, P.E. Raad, K.P. Pipe, A. Shakouri, R.J. Ram, J.A. Hudgings. CCD-based thermoreflectance microscopy: principles and applications. *Journal of Physics D: Applied Physics* **42**(143001), 2009.

[2] S. Grauby, B.C. Forget, S. Holé, D. Fournier. High resolution photothermal imaging of high frequency phenomena using a visible charge coupled device camera associated with a multichannel lock-in scheme. *Review of Scientific Instruments* **70**(9):3603–3608, 1999.

[3] S.B. Riffat, X. Ma. Thermoelectrics: a review of present and potential applications. *Applied Thermal Engineering* **23**(8):913 – 935, 2003.

[4] L.E. Bell. Cooling, heating, generating power, and recovering waste heat with thermoelectric systems. *Science* **321**(5895):1457–1461, 2008.

[5] A. Shakouri. Nanoscale thermal transport and microrefrigerators on a chip. *Proceedings of the IEEE* **94**(8):1613–1638, 2006.

[6] B. Vermeersch, J. Christofferson, K. Maize, A. Shakouri, G. De Mey. Time and frequency domain CCD-based thermoreflectance techniques for high-resolution transient thermal imaging. In *Proceedings of IEEE 26th SEMI-THERM, Santa Clara, Feb 23-25*, pp. 228–234, 2010.